

Structural, electronic, optical, mechanical and magnetic properties of Co_2CrZ ($Z = \text{As, B, Ga, Pb}$) full-Heusler compounds

P. Singh^a, S. Mahla^{b,*}, M. G. Chaudhary^c, R. Agrawal^d, C. Singh^a, A. S. Verma^{e,f,*}

^aDepartment of Physics, Agra College, Agra 282002 India

^bDepartment of Physics, GDC Memorial College, Bahal, Bhiwani 127028 India

^cDepartment of Physics, SRM Institute of Science & Technology, Delhi-NCR Campus, Modinagar, Ghaziabad 201204 India

^dDepartment of Computer Engineering and Applications, G. L. A. University, Mathura 281406, India

^eDivision of Research & Innovation, School of Applied and Life Sciences, Uttaranchal University, Dehradun, Uttarakhand 284007 India

^fUniversity Centre for Research & Development, Department of Physics, Chandigarh University, Mohali, Punjab 140413 India

Two separate computational algorithms have been used in the current investigation of Full-Heusler compounds. One is the pseudo-potential approach used in the Atomistic Tool Kit-Virtual Nanolab, while the other is FP-LAPW method as implemented in WIEN2k. In the computational code, these compounds exhibit metallic character in both the majority and minority spin channels. According to the WIEN2k and ATK-VNL codes, the computed magnetic moments of these compounds Co_2CrZ ($Z = \text{As, B, Ga, and Pb}$) are $4.93 \mu_B$ and $5.02 \mu_B$, $3.00 \mu_B$ and $3.08 \mu_B$, $3.02 \mu_B$ and $3.16 \mu_B$, and $4.07 \mu_B$ and $4.30 \mu_B$, respectively. Between the estimated value and the Slater-Pauling rule, we discovered excellent agreement. These compounds' optical characteristics include reflectivity, refractive index, excitation coefficient, and absorption coefficient, among others. An analysis has been done on the electron energy loss and optical conductivity. Both the electron energy-loss function and the absorption coefficient increase as the energy value increases. As per the results of elastic properties, Co_2CrZ compounds with $Z = \text{As, Pb}$ are ductile by nature, whereas those with $Z = \text{B, Ga}$ are brittle. Co_2CrZ ($Z = \text{As, B, Ga, and Pb}$) compounds exhibit metallic behaviour when their Cauchy pressure ($\text{CP} = C_{12} - C_{44}$) value is positive.

(Received April 18, 2023; Accepted July 28, 2023)

Keywords: Half metal ferromagnetic, Band gap, Spintronics, Magnetic moment, Elastic constant

1. Introduction

The Heusler compound is named after its discoverer, Friedrich Heusler [1] in 1903. He was a German chemist and mining engineer. Friedrich discovered in his invention that the three non-magnetic elements Cu, Mn and Al confirm magnetism at room temperature [2] as a compound. Thereafter, in the year of 1983, the concept of Half-metallic ferromagnetism (HMF) was suggested by de Groot [3-5]. They predicted that due to the up spin of electrons the compound shows metallic nature and down spin is semiconducting. Its Half-metallic ferromagnetism (HMF) represents the spin polarization at the Fermi level [6-8]. Coe et al. [9] have observed from their study that the quasi-metallic ferromagnetism of the material is due to electron spins rather than its charges. Vermehl et al. [10] have investigated that Co_2FeSi exhibits a very high Curie temperature of 1100K with $6\mu_B$ magnetic moment. Kandpal et al. [11] presented their results that Co_2FeSi shows a band gap at the Fermi level using first principle. Half Metal Ferromagnetism (HMF) Heusler compounds have also been shown by Ishida et al [12]. The physical properties of Co_2MnAl thin films have been studied by Hashemifer et al. [13] and found that Mn maintains half

* Corresponding author: ajay_phy@rediffmail.com
<https://doi.org/10.15251/JOR.2023.194.387>

the metallicity by its strong surface subsurface using the density function theory. Telling et al. [14] performed their experiment on Co₂ based Heusler compounds which showed the origin of magnetic moments and band gap. Magnetic Tunnel Junction for Co₂MnAl was developed by Sakuraba et al. [15] grew epitaxially with 0.2 nm width and found to have very large tunneling magneto-resistance (TMR). Uematsu et al. [16] have scrutinized that the Co₂CrGa compound has a static magnetic moment of 3.01 μ_B at 4.2 k and obeys the Slater–Pauling rule, that the total magnetic moment per unit cell is equal to the difference between the total number of valence electrons and 24. Miura et al. [17] has also been willful that Co-based Full Heusler compounds show the deeds of half-metallic ferromagnets. In the new era, magneto electronics attracted research based on ferromagnetic materials. Semi-metallic ferromagnetism is a new class of materials based on the spin of the electron. The concept of spintronics has been applied in many magneto electronics such as magnetic memory devices, magnetic sensors, tunnel junctions, Very useful in the increase in data processing speed increases the integration speed and it also reduces the power consumption [18–21]. This paper presents the results of all fundamental physical properties of Co₂CrZ (Z = As, B, Ga, Pb) compounds using the WIEN2k code and the Atomic Tool Kit-Virtual Nanolab (ATK-VNL) code.

2. Computational details

The computational code WIEN2k [22] is based on FP-LAPW [23] which is used to study the physical fundamental properties of full Heusler alloys. We choose the Perdew, Burke and Ernzerhof (PBE) approximation [24] suitable for synchronizing the exchange and correlation potential energies. Generalized-gradient approximation (GGA) [25] was used for the optimization of parameters such as RK max, K-point, lattice constant and optimized energy. All calculations are performed using the spin orbit coupling effect. The WIEN2k code calculates accurate electronic structure calculations for solids. The cut off parameter (energy between the two states) was set to -6.0Ry. In these two states, the core states are treated relativistically and the valence states are treated in a semi-relativistic manner. For this code, we first set 1000 k-points in the Brillouin zone. The figure of k-points was increased for the estimate of optical properties up to 10000. The value of $R_{MT}K_{max}$ (cutoff parameter) is set to 7.0, which is used to control the size of the basis set. Here R_{mt} is used for the smallest radius plane wave of the muffin-tin sphere and K_{max} is applied for the maximum modulus of the reciprocal lattice vector used in the expansion of the flat wave function. An energy convergence criterion is set 0.0001Ry. The worth of angular momentum l_{max} is taken to be 10, which is used to expand the spherical harmonics in the nuclear region. The charge density and potential in the central region were detailed as an excitable series with wave vector up to $G_{max} = 10$. For each nuclear muffin tin sphere radii (R_{MT}) are tabulated in Table 1.

Table 1. Muffin tin radius (R_{MT}) for Co₂CrZ (Z = As, B, Ga, Pb).

R_{MT} (a.u.)	Compounds			
	Co ₂ CrAs	Co ₂ CrB	Co ₂ CrGa	Co ₂ CrPb
CO	2.41	2.18	2.18	2.35
Cr	2.29	2.08	2.08	2.35
Z	2.29	1.81	2.08	2.47

A computational code based on the ATK-VNL pseudo-potential method, carried out in the outline of density functional theory and has also been applied to the study of the above physical fundamental properties of Full Heusler alloys [26]. The Pulley mixer algorithm [27] was applied to investigate the electronic and magnetic properties of Co₂CrZ (Z = As, B, Ga, Pb) using first-principles calculations. For the expansion of the electron wave function, we used a double-zeta (ζ) have used polarized basis sets and GGA (generalized-gradient approximation). The formations are

allowed to optimize until each atomic force convergence criterion is achieved at 0.05 eV/Å and the maximum strain is 0.05 eV/Å³. A step size of 0.2 Å is fixed for the optimization to perform a maximum of 200 steps. Convergence is accomplished by determining the mesh cutoff energy based on convergence theory and its calculation at 150 Ryd has been estimated. For spin polarization, up and down states have been chosen for the atoms. We have used a 10 x 10 x 10 Monkhorst-Pack k-mesh [28] for Brillouin zone sampling to maintain a balance between computational time and accuracy results. In addition, for structure optimization, No constraints are applied in the x, y and z directions.

3. Results and discussions

3.1. Structural parameters

Herein, we found the cubic lattice structure of L2₁ (space group: 225 Fm-3m) formed by four penetrating FCC-lattices with atomic positions at X₁ (1/4, 1/4, 1/4), X₂ (3/4, 3/4, 3/4), Y (1/2, 1/2, 1/2) and Z (0, 0, 0). Where X and Y atoms are transition metals and Z is a main group metal or semimetal. The equation of state given by Murnaghan [29] gives the values of total energy and pressure as a function of volume:

$$E(V) = E_0 + \left[\frac{BV}{B_p} \left(\frac{1}{(B_p - 1)} \left(\frac{V_0}{V} \right)^{B_p} + 1 \right) - \frac{BV_0}{(B_p - 1)} \right]$$

$$P(V) = \frac{B}{B_p} \left\{ \left(\frac{V_0}{V} \right)^{B_p} - 1 \right\}$$

where,

$$\text{Pressure (P)} = -\frac{dE}{dV} B_p = -V \frac{dP}{dV} = V \frac{d^2E}{dV^2}$$

In the above equations E₀ is the energy minimum at T = 0K, B is the bulk modulus, B_p is the pressure derivative of the bulk modulus and V₀ is the equilibrium volume. The structural optimization for all four compounds is shown in Figure 1. If we analyze the lattice constants obtained from both the codes WIEN2k and ATK-VNL, we see that the values of lattice constants of WIEN2k are slightly less than those of ATK-VNL. But this difference is reversed in the case of bulk modulus. This means that the bulk modulus of WIEN2k is slightly higher than the bulk modulus of ATK-VNL and values are presented in Table 2.

Table 2. Optimized parameters of Co₂CrZ (Z = As, B, Ga, Pb).

Compounds	Lattice Constants a ₀ (Å)		Bulk modulus (GPa)		Equilibrium Energy (Ry)	Pressure derivative WIEN2k
	Calculated		Calculated			
	WIEN2k	ATK	WIEN2k	ATK		
Co ₂ CrAs	5.787	5.859	225	206	Co ₂ CrAs	5.787
Co ₂ CrB	5.385	5.470	270	200	Co ₂ CrB	5.385
Co ₂ CrGa	5.723	5.794	203	180	Co ₂ CrGa	5.723
Co ₂ CrPb	6.099	6.120	220	181	Co ₂ CrPb	6.099

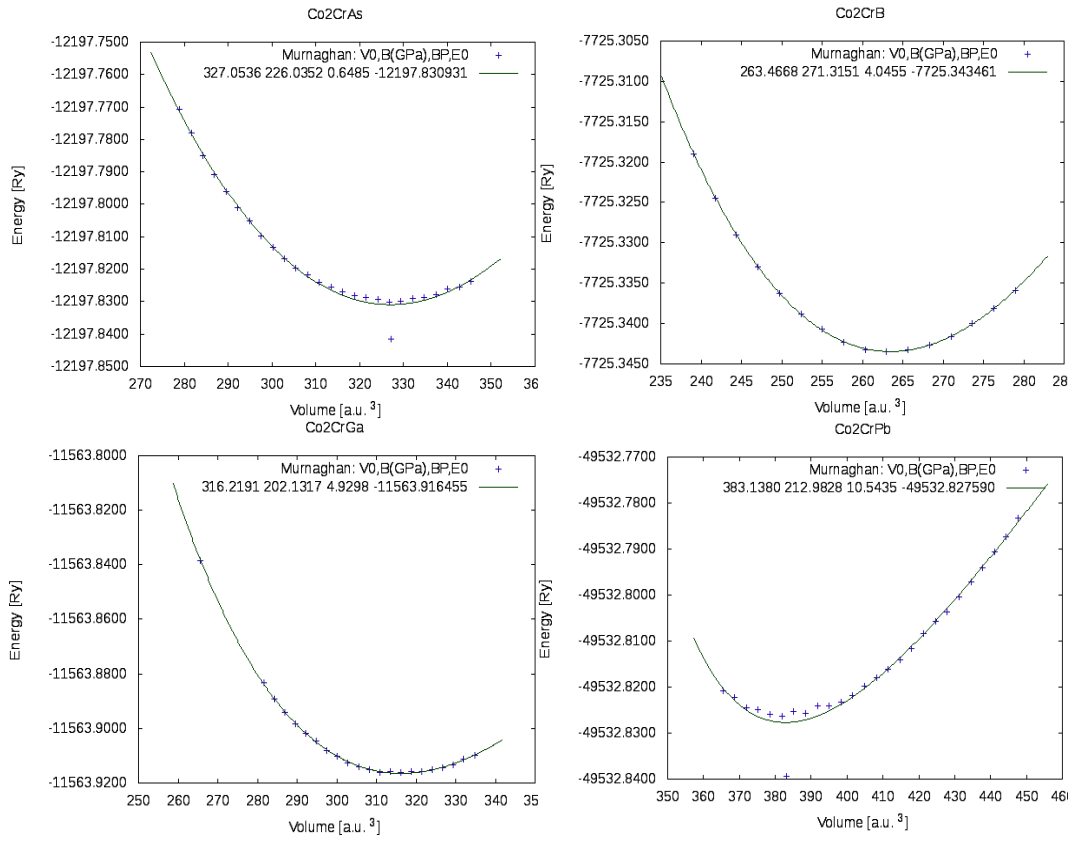


Fig. 1. Volume optimization for lattice parameters.

3.2. Electronic and magnetic properties

The spin of an electron is responsible for the magnetic moment in a material. If the up spin state shows no band gap in Heusler compounds and the down spin state has a finite band gap, then the material is a half-metallic ferromagnetic showing 100% spin polarization at the Fermi level. This phenomenon is known as spin polarization. Today's spintronics is a new growing area of research with many applications. Various magneto-electronic and high processing devices have been developed using the concept of spintronics. These devices reduce power consumption and also reduce heat dissipation. Spin polarized computation of Co_2CrZ ($Z = \text{As, B, Ga, Pb}$) compounds have been carried out on optimized lattice parameters within the generalized-gradient approximation (GGA).

$$P_n = \frac{n_{\uparrow} - n_{\downarrow}}{n_{\uparrow} + n_{\downarrow}}$$

If either $n_{\uparrow} = 0$ or $n_{\downarrow} = 0$, then $P_n = 1$ or -1 . This means, if spin up or down is present then the spin polarization is 100%. Materials of this type are known as half-metal ferromagnetic. If the value of P_n vanishes then the material is paramagnetic or anti-ferromagnetic even below the magnetic transition temperature. The energy gap is the difference between the highest energy point in the valence band region and the lowest empty energy point in the conduction band. Energy gap from DOS and band structure studies of Co_2CrZ ($Z = \text{As, B, Ga, Pb}$) compounds show that no band gap exists in the up or down spin channels. All the four listed compounds here show the metallic nature of the material. Both the computational codes show zero band gaps in spin up or spin down state.

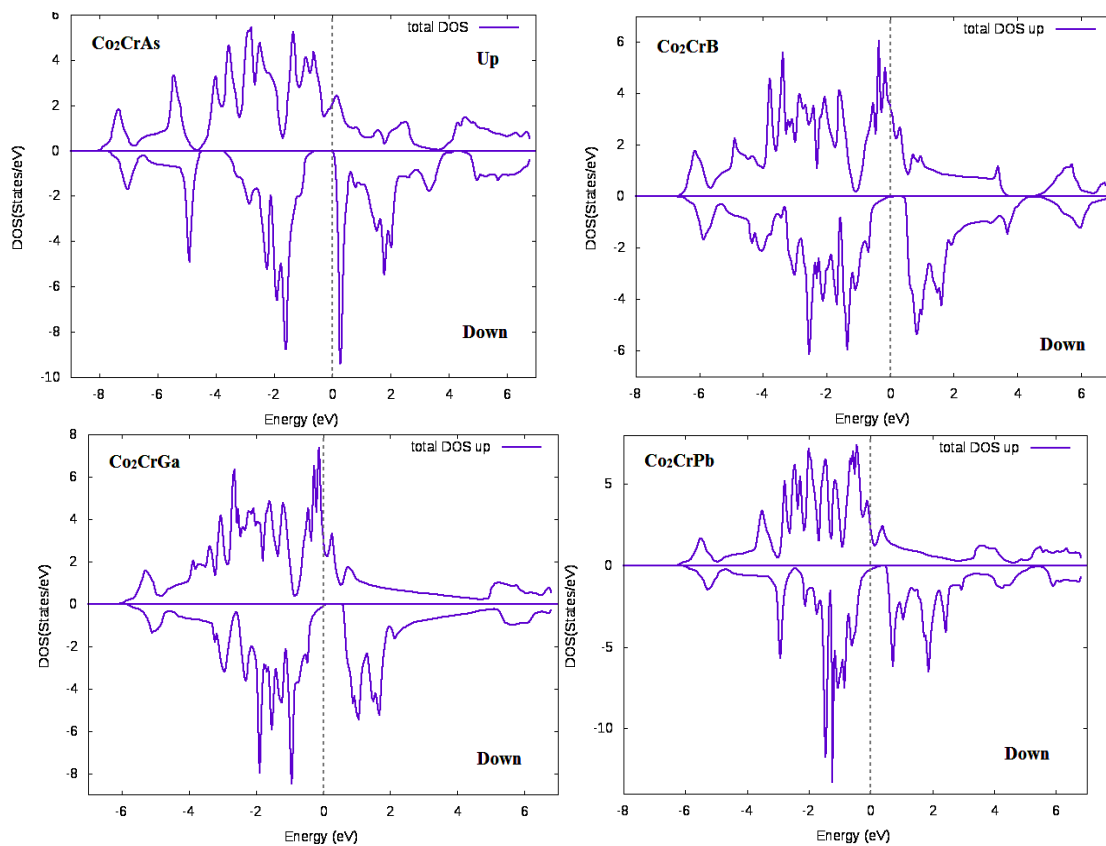


Fig. 2. Density of states of Co_2CrZ ($Z = \text{As}, \text{B}, \text{Ga}, \text{Pb}$) using the WIEN2K code.

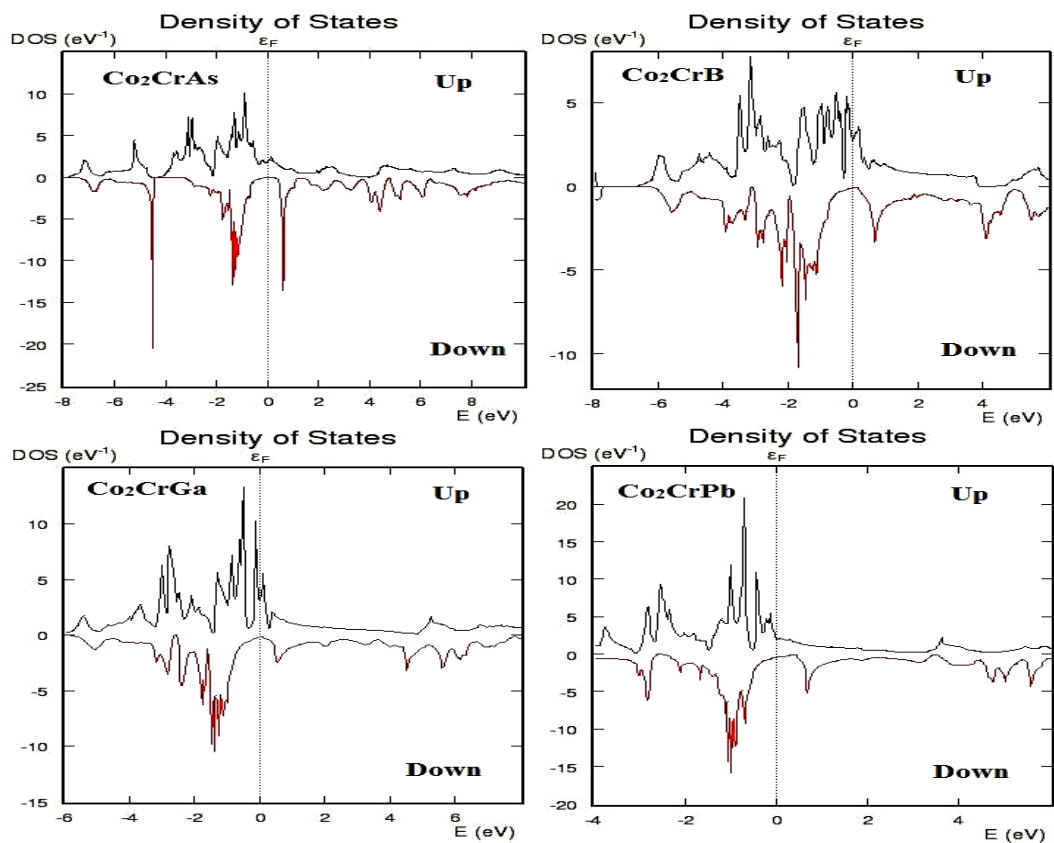


Fig. 3. Density of states of Co_2CrZ ($Z = \text{As}, \text{B}, \text{Ga}, \text{Pb}$) using the ATK-VNL code.

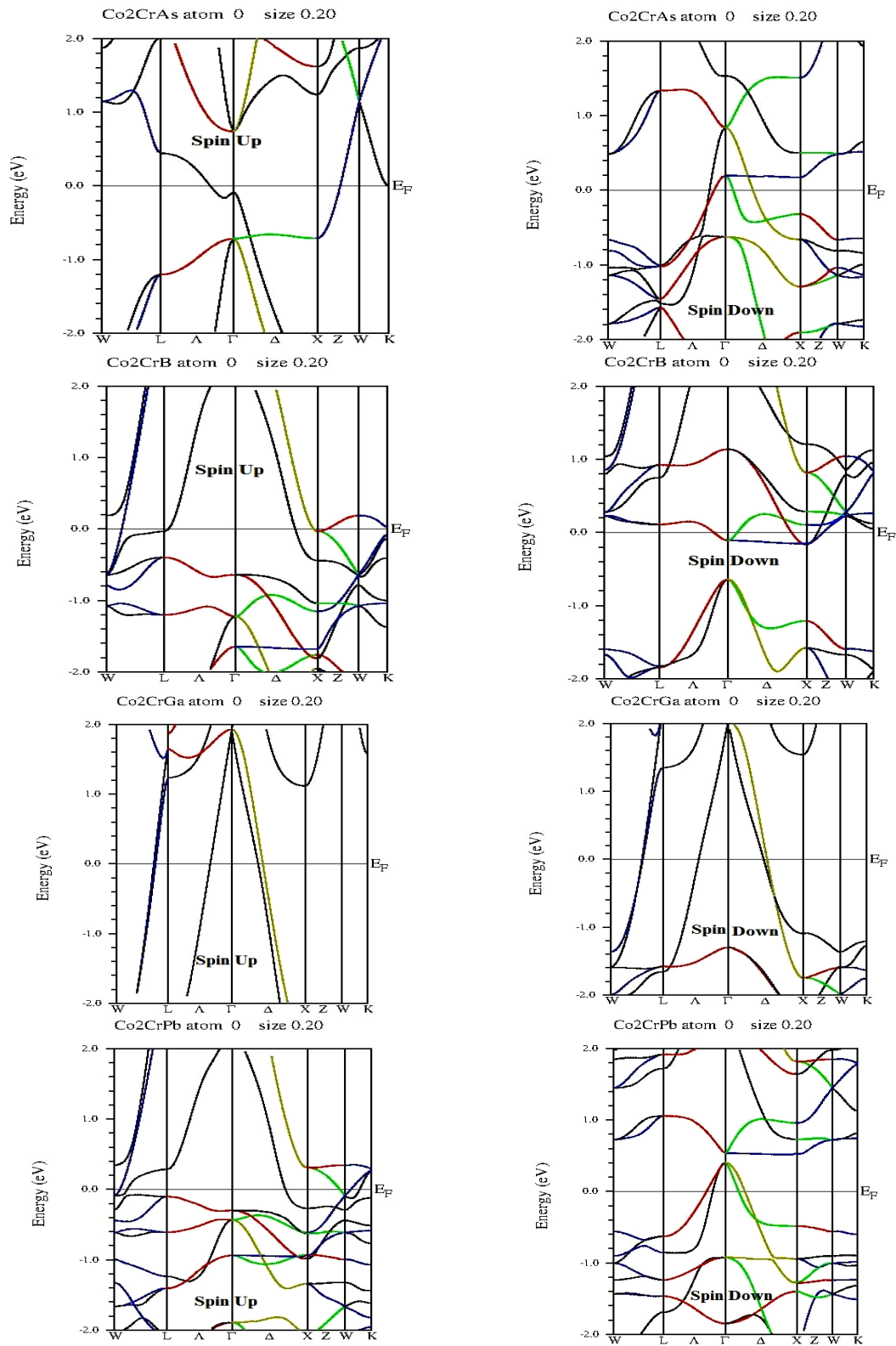
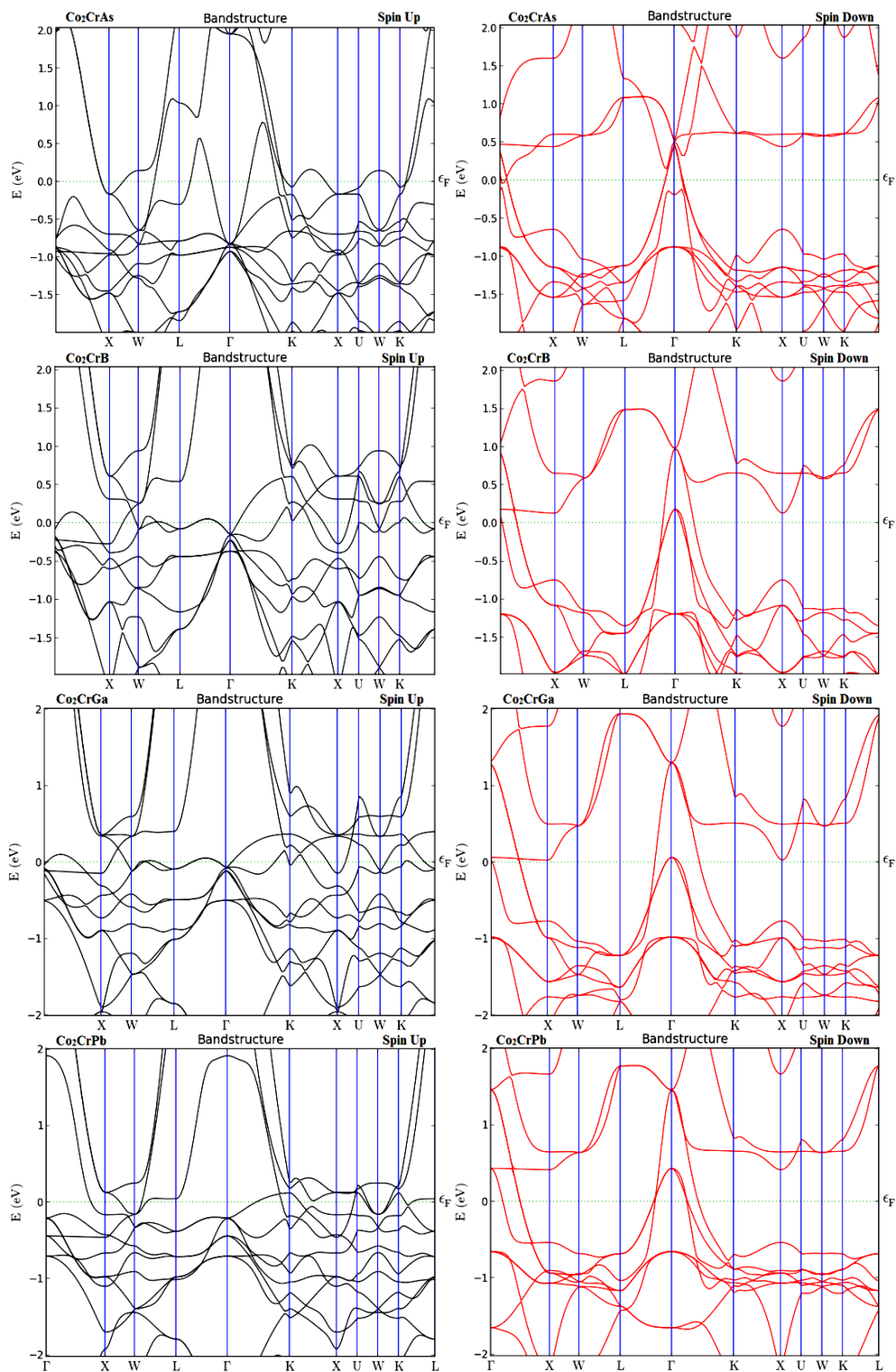


Fig. 4. Band structure of Co_2CrZ ($Z = \text{As, B, Ga, Pb}$) using the WIEN2K code.

Table 3. Band gap and spin polarization of Co_2CrZ ($Z = \text{As}, \text{B}, \text{Ga}, \text{Pb}$).

Compound	Band gap E_g (eV)				Spin polarization	
	WIEN2k		ATK		WIEN2k	ATK
	Up spin	Down spin	Up spin	Down spin		
Co_2CrAs	0.0	0.0	0.0	0.0	P_n vanishing	P_n vanishing
Co_2CrB	0.0	0.0	0.0	0.0	P_n vanishing	P_n vanishing
Co_2CrGa	0.0	0.0	0.0	0.0	P_n vanishing	P_n vanishing
Co_2CrPb	0.0	0.0	0.0	0.0	P_n vanishing	P_n vanishing

Fig. 5. Band structure of Co_2CrZ ($Z = \text{As}, \text{B}, \text{Ga}, \text{Pb}$) using the ATK-VNL code.

The Slater–Pauling rule gives us a direct relationship between the total number of valence electrons (Z_t) and the total spin magnetic moment (M_t) when we study Heusler alloys. The difference between the total number of valence electrons and 24 gives the total magnetic moment of the Full Heusler compound [30–31]. Here the total number of valence electrons of the compounds Co_2CrZ ($Z = \text{As, B, Ga, Pb}$) are 29, 27, 27 and 28. Therefore, according to the Slater–Pauling rule, their magnetic moments are 5, 3, 3 and 4 μ_B respectively. The compound Co_2CrAs exhibits the highest magnetic moment because 29 valence electrons are present in that compound. The Curie temperature is also linked to the total number of valence electrons. The difference between the total valence electrons and 24 is an integral multiple of 175 K, gives the total value of the Curie temperature. So, the Curie temperature of the compound Co_2CrZ ($Z = \text{As, B, Ga, Pb}$) are 875, 525, 525 and 700 K respectively. From Table 4, we see that the values of magnetic moments per unit cell by the computational codes WIEN2k and ATK-VNL are almost equivalent to each other and their values are also almost equivalent to the Slater–Pauling rule. So, we summarize that these compounds have good agreement with the Slater–Pauling rule. The values generated by the pseudo-potential method (ATK-VNL) are slightly higher than those produced by the full-potential method (WIEN2k). Co_2CrZ ($Z = \text{As, B, Ga, Pb}$) have been obtained using the FP-LAPW method implemented in WIEN2k and the pseudo-potential method implemented in ATK-VNL within GGA for the exchange correlation functions are tabulated in Table 4.

Table 4. Total magnetic moment of Co_2CrZ ($Z = \text{As, B, Ga, Pb}$).

Compound	Z_t	Magnetic moment (μ_B)		
		WIEN2k	ATK	Slater-Pauling ($Z_t - 24$)
Co_2CrAs	29	4.93	Co_2CrAs	29
Co_2CrB	27	3.00	Co_2CrB	27
Co_2CrGa	27	3.02	Co_2CrGa	27
Co_2CrPb	28	4.07	Co_2CrPb	28

3.3. Optical properties

One of a material's most critical characteristics is its optical properties. The complex dielectric function may be used to characterise the linear response of the short wave vector optical response of a material when electromagnetic radiation is impinged on it. This complex dielectric function can be written [32] as, $\epsilon(\omega) = \epsilon_1(\omega) + i\epsilon_2(\omega)$.

Where ($\epsilon_1(\omega)$) is the real part of the complex dielectric function, describing the polarization of the material; When electric field is applied and ($\epsilon_2(\omega)$) The imaginary part of the complex dielectric function gives the value of absorption in a substance or loss of energy in the medium. We choose the inter-band region to study the optical properties. The optical spectra for different optical properties are shown in Figure 6(Ah). The main peaks of the imaginary part of the dielectric function are obtained in the infrared region from 0.08 to 0.30eV. After that, the imaginary part of the dielectric function decreases rapidly and some small peaks are observed near the field of view. The real of the complex dielectric functions ($\epsilon_1(\omega)$) and the imaginary part ($\epsilon_2(\omega)$) of the zero frequency values 403.96 and 403.96, 283.72 and 104.89, 293.6 and 107.97, 279.79 and 97.68 for the compound Co_2CrZ ($Z = \text{As, B, Ga, Pb}$) were examined from figure 6(a) and 6(b), respectively. Figure 6(c) gives a graphical representation of the optical conductivity showing sharp peaks in the visible region and the highest sharp peak at 2.27eV is obtained by Co_2CrB representing higher conduction of electrons than other compounds. The photon absorption values increase as we move from the infrared to the ultraviolet range, as seen from Fig. 6(d). A fast moving electron loses its energy on passing through a medium and this loss can be calculated by graphing the electron energy-loss function.

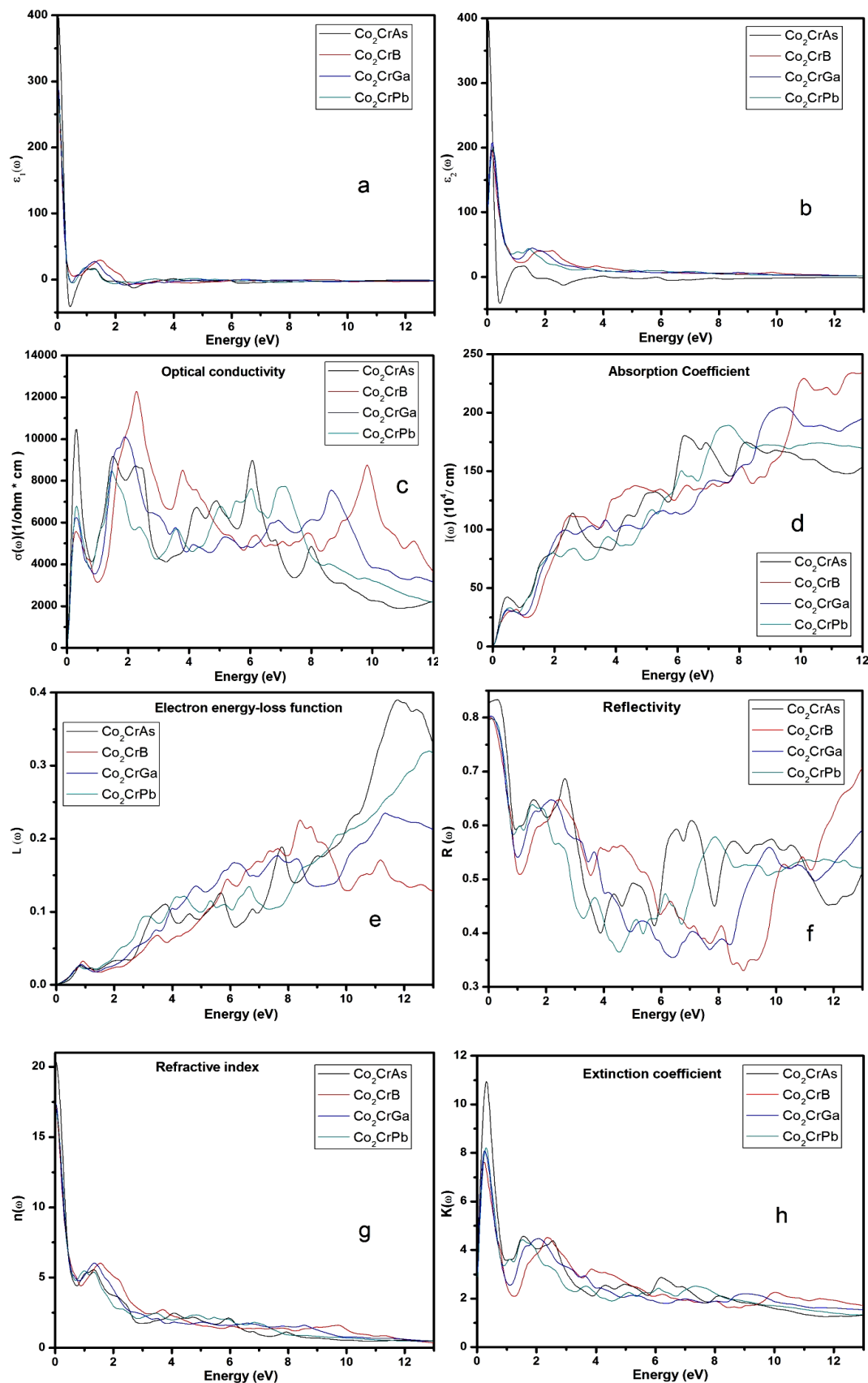


Fig. 6. The calculated optical parameters are (a) the real part of the dielectric function, (b) the imaginary part of the dielectric function, (c) the optical conductivity, (d) the absorption coefficient, (e) the electron energy-loss function, (f) the reflectivity, (g) Refractive index and (h) extinction coefficient for Co_2CrZ ($Z = \text{As, B, Ga, Pb}$).

The value of the electron energy-loss function also increases as we increase the value of energy and at energy 11.76 eV Co₂CrAs shows maximum electron energy loss as shown in Fig. 6(e). Reflectance determines the material's ability to reflect what fraction of electromagnetic radiation is incident on its surface. Figure 6(f), represent the values of zero frequency reflectivity which are 0.827, 0.797, 0.800 and 0.795 for the compounds Co₂CrZ (Z = As, B, Ga, Pb), respectively. Absorption and reflection are inversely proportional to each other in the same period. The plasma frequency is the frequency associated with the plasma resonance at which the sharp peaks are associated. As the frequency is above the plasma frequency the material shows dielectric behavior and below which the material shows metallic behavior. Refractive index has a wide field of application such as dispersive power of prism, focusing power of lens, light guide, and critical angle for total internal reflection etc. The zero frequency values of refractive index for the compound Co₂CrZ (Z = As, B, Ga, Pb) were obtained as 20.427, 17.120, 17.413 and 16.973, respectively. Figure 6(h) gives a graphical representation of the extinction coefficient spectrum. In the infrared region between 0.12 to 0.54eV region, a notable sharp peak at 0.33 is obtained by the Co₂CrAs compound and then the value of the extinction coefficient decreases. A small broad peak is observed from 1.46 to 2.59eV further near the visible region and the value further decreases in the ultraviolet region 54eV and then the value of extinction coefficient decreases.

3.4. Elastic properties

An externally applied force deforms a solid object and an internal force opposes this deformation. The value of deformation of a solid depends on the elastic properties of the material, which is calculated here using the first principle method. Of the six independent constants, three of the lesser elastic constants C_{11} , C_{12} and C_{44} are used to determine the cubic crystal elasticity. These three reduced elastic constants provide us the information of the structure stability, mechanical properties, bond index and anisotropy of the material. Cubic crystals must satisfy the conventional mechanical stability condition of the elastic constant, which is set out in [33] below.

$$C_{11} - C_{12} > 0, C_{11} > 0, C_{11} + 2C_{12} > 0, C_{44} > 0, C_{12} < B < C_{11}$$

The anisotropic factor is used to determine the structural stability, which is denoted by 'A'. If the value of 'A' is equal to one then the material is isotropic otherwise the material is anisotropic. A property of a material which depends on the direction is known as anisotropic. Anisotropic is related to the low elastic constant.

$$A = \frac{2C_{44}}{C_{11} - C_{12}}$$

The Bond index can determine the toughness and ductility of a material using the Cauchy pressure, which is expressed as $CP = C_{12} - C_{44}$. If the value of Cauchy pressure is positive, then the material is of metallic and ductile nature. Furthermore, if the value is negative, then the material is nonmetallic and ductile in nature. Pugh's ratio B/G is used to determine whether a material is brittle or ductile. If B/G ratio is less than 1.75 then the material is brittle type otherwise it is ductile. The mechanical properties of compounds are determined by the Voigt–Ries–Hill (VRH) averaging method [34] of the bulk modulus (B), Young's modulus (E), shear modulus (G) and Poisson's ratio (ν). Using the elastic constants can be expressed as formulas for B, E, G and V.

$$B = B_V = B_R = \frac{C_{11} + 2C_{12}}{3}$$

$$G = \frac{G_V + G_R}{2}$$

$$G_V = \frac{C_{11} - C_{12} + 3C_{44}}{5}$$

$$G_R = \frac{5C_{44}(C_{11} - C_{12})}{[4C_{44} + 3(C_{11} - C_{12})]}$$

(V = Voigt and R = Reiss)

The hardness of a material can be determined by the Young's modulus. It can be calculated in terms of b and g.

$$E = \frac{9BG}{3B + G}$$

The value of the Poisson's ratio are premeditated in terms of b and g. Poisson's ratio values for most materials lie between 0 - 0.5.

$$\nu = \frac{3B - 2G}{2(3B + G)}$$

Here, we have used a pseudo-potential method performed in the framework of density functional theory (DFT) using the Atomic Tool Kit-Virtual Nanolab (ATK-VNL) package. All the results from this code are gathered in Table 5.

Table 5. Elastic constants and bulk modulus B (GPa), shear modulus G (GPa), Young's modulus E (GPa), B/G values, Poisson's ratio (ν) and anisotropy factor (A) of Co_2CrZ (Z= As, B, Ga, Pb) compounds.

Compound	Elastic constant			B (GPa)	G (GPa)	E (GPa)	B/G	V	A
	C_{11}	C_{12}	C_{44}						
Co_2CrAs	255.80	181.22	83.61	206.08	60.47	105.51	3.41	0.41	2.24
Co_2CrB	167.54	217.68	22.31	200.97	47.39	-78.48	4.24	0.57	-0.89
Co_2CrGa	159.19	191.05	116.71	180.43	6.79	-49.23	26.69	0.54	-7.33
Co_2CrPb	213.68	165.76	130.69	181.73	67.49	68.85	2.69	0.44	5.45

From Table 5, we see that the conventional mechanical stability condition $C_{11} - C_{12} > 0$, $C_{11} > 0$, $C_{11} + 2C_{12} > 0$, $C_{44} > 0$, $C_{12} < B < C_{11}$ for the compound Co_2CrZ (Z= As, Pb) is satisfied. But for the compound Co_2CrB and Co_2CrGa this condition is not satisfied. The results for the anisotropic constant 'A' are deviate from one for all the four compounds. Therefore, we conclude that the compound Co_2CrZ (Z = As, B, Ga, Pb) is anisotropic in nature. The Poisson's value for Co_2CrZ (Z = As, Pb) ranges from zero to 0.5. The results in Table 5 reveal that for Co_2CrZ (Z = As, Pb) compounds the Pugh's ratio B/G is greater than 1.75, so these materials are ductile in nature. But Co_2CrB and Co_2CrGa are brittle in nature. The values of Cauchy pressure (CP = $C_{12} - C_{44}$) accumulated by Table 5 for all these compounds Co_2CrZ (Z= As, B, Ga, Pb) showing metallic nature.

4. Summary and conclusions

We performed ab initio calculations for the electrical, optical, elastic, and magnetic properties of the Full Heusler compounds Co_2CrZ (Z = As, B, Ga, and Pb). A pseudorandomization within the generalized-gradient approximation (GGA) is implemented in the Atomistic Tool Kit-Virtual NanoLab (ATK-VNL) within the generalised-gradient approximation (GGA) for exchange and correlation functions. The other computational code is the full potential linearized augmented plane wave (FP-LAPW) method implemented in WIEN2k. According to the study, both computational algorithms have detected the metallic character of these molecules. Slater-Pauling behaviour and computed magnetic moments per unit cell agree well. The terms reflectance, refractive index, excitation coefficient, absorption coefficient, etc. are used to describe the optical spectra of these substances. The optical conductivity and electron energy loss have been

analyzed. With the increase in energy the values of absorption coefficient and electron energy-loss functions increase. The predicted results suggest that the compound Co_2CrZ ($Z = \text{As, B, Ga, Pb}$) is not suitable for spintronics applications. The elastic properties results show that Co_2CrZ ($Z = \text{As, Pb}$) compounds are ductile in nature and Co_2CrZ ($Z = \text{B, Ga}$) are brittle in nature.

References

- [1] Fr. Heusler, *Verh. Dtsch. Phys. Ges.* 5 (1903) 219.
- [2] Fr. Heusler and E. Take, *Trans. Faraday Soc.* 8 (1912) 169-184;
<https://doi.org/10.1039/tf9120800169>
- [3] R.A. De Groot, F.M. Muller, P. G. Van Engen and K.H.J. Buschow, *Phys. Rev. Lett.* 50 (1983) 2024-2027; <https://doi.org/10.1103/PhysRevLett.50.2024>
- [4] Sukhender, L. Mohan, S. Kumar, D. Sharma, A. S. Verma, *East Eur. J. Phys.* 2 (2020) 69-80.
- [5] Sukhender, Pravesh, L. Mohan, A. S. Verma, *East Eur. J. Phys.*, 3 (2020) 99-110.
- [6] Sukhender, Pravesh, L. Mohan, A. S. Verma, *East Eur. J. Phys.* 3 (2020) 111-121.
- [7] Sukhender, L. Mohan, A. S. Verma, *East Eur. J. Phys.*, 4 (2020) 51-62.
- [8] S. A. Wolf, D. D. Awschalom, R. A. Buhrman, J. Daughton, S. von Molnar, M. L. Roukes, A. Y. Chtchelkanova and D. M. Treger, *Science* 294 (2001) 1488-1495;
<https://doi.org/10.1126/science.1065389>
- [9] J. M. D. Coey, M. Venkatesan and M. A. Bari, *Half-Metallic Ferromagnets*. Springer-Verlag, Heidelberg, 595 (2002) 377-396; https://doi.org/10.1007/3-540-45649-X_15
- [10] S. Wurmehl, G. H. Fecher, H. C. Kandpal, V. Ksenofontov, C. Felser, H. Ji Lin, and J. Morais, *Phys. Rev. B* 72 (2005) 184434; <https://doi.org/10.1103/PhysRevB.72.184434>
- [11] H. C. Kandpal, G. H. Fecher, C. Felser, and G. Schonhense, *Phys. Rev. B*, 73 (2006) 094422-094433.
- [12] S. Ishida, S. Fujii, S. Kashiwagi and S. Asano, *J. Phys. Soc. Jap.* 64 (1995) 2152-2157;
<https://doi.org/10.1143/JPSJ.64.2152>
- [13] S. J. Hashemifar, P. Kratzer and M. Scheffler, *Phys. Rev.*, 94 (2005) 096402-096405;
<https://doi.org/10.1103/PhysRevLett.94.096402>
- [14] N. D. Telling, P. S. Keatly, G. van der Lann, R. J. Hicken, E. Arenholz, Y. Sakurba, M. Oogane, Y. Ando, K. Takanashi, A. Sakuma and T. Miyazaki, *Phys. Rev. B* 78 (2008) 184438-1884445; <https://doi.org/10.1103/PhysRevB.78.184438>
- [15] Y. Sakuraba, J. Nakata, M. Oogane, Y. Ando, H. Kato, A. Sakuma and T. Miyazaki, *Appl. Phys. Letts.*, 88 (2006) 022503-022506; <https://doi.org/10.1063/1.2162867>
- [16] R.Y. Umetsu, K. Kobayashi, R. Kainuma, A. Fujita, K. Fukamichi, K. Ishida, A. Sakuma, *Appl. Phys. Lett.* 85 (2004) 2011-2013; <https://doi.org/10.1063/1.1790029>
- [17] Y. Miura, K. Nagao and M. Shirai, *Phys. Rev. B* 69 (2004) 144413.
- [18] H. Ohno, *Science* 281(1998) 951-956; <https://doi.org/10.1126/science.281.5379.951>
- [19] R. J. Soulen Jr., J. M. Byers, M. S. Osofsky, B. Nadgorny, T. Ambrose, S. F. Cheng, P. R. Broussard, C. T. Tanaka, J. Nowak, J. S. Moodera, A. Barry and J. M. D. Coey, *Science* 282 (1998) 85-88; <https://doi.org/10.1126/science.282.5386.85>
- [20] J. S. Moodera, L. R. Kinder, T. M. Wong and R. Meservey, *Phys. Rev Lett.* 74 (1995) 3273-3276; <https://doi.org/10.1103/PhysRevLett.74.3273>
- [21] B. Dieny, V. S. Speriosu, S. S. P. Parkin, B. A. Gruney, D. R. Wilhoit and D. Mauri, *Phys. Rev. B Condens. Matter.* 43 (1991) 1297-1300; <https://doi.org/10.1103/PhysRevB.43.1297>
- [22] P. Blaha, K. Schwarz, G. K. H. Madsen, D. Kvasnicka and J. Luitz in *WIEN2k, An Augmented Plane Wave + Local Orbitals Program for Calculating Crystal Properties*, edited by K Schwarz (Technical Universitatwien, Austria, (2001), ISBN 3-9501031-1-2.
- [23] S. E. Kulkova, S. V. Eremeev, T. Kakeshita, S. S. Kulkov, and G. E. Rudenski, *Mater. Trans.* 47 (2006) 599- 606; <https://doi.org/10.2320/matertrans.47.599>

- [24] J. P. Perdew, K. Burke and M. Ernzerhof, Phys. Rev. Lett. 77 (1996) 3865-3868; <https://doi.org/10.1103/PhysRevLett.77.3865>
- [25] D. Singh, Planes Waves, Pseudo-Potentials and the LAPW Method, Kluwer Academic Publishers, Boston, Dordrecht, London, 1994.
- [26] Atomistix ToolKit-Virtual Nanolab (ATK-VNL), QuantumWise Simulator, Version. 2014.3.[Online]. Available: <http://quantumwise.com/>
- [27] P. Pulay, J. Comput. Chem. 3 (1982) 556-560; <https://doi.org/10.1002/jcc.540030413>
- [28] H. J. Monkhorst, and J. D. Pack, Phys. Rev. B 13 (1976) 5188-5192; <https://doi.org/10.1103/PhysRevB.13.5188>
- [29] F. D. Murnaghan, Proc. Natl. Acad. Sci. U. S. A. 30 (1944) 244-247; <https://doi.org/10.1073/pnas.30.9.244>
- [30] S. Qi, J. Shen, C. H. Zhang, Mater. Chem. Phys, 164 (2015) 177-182; <https://doi.org/10.1016/j.matchemphys.2015.08.040>
- [31] S. Skaftouros, K. Özdoğan, E. Şaşıoğlu, I. Galanikis, Phys. Rev. B, 87 (2013) 024420; <https://doi.org/10.1103/PhysRevB.87.024420>
- [32] A.S. Verma, R. Gautam, P. Singh, S. Sharma, S. Kumari, Mater. Sci. Eng. B 205 (2016) 18-27; <https://doi.org/10.1016/j.mseb.2015.11.010>
- [33] M. Afsari, A. Boochani, M. Hantezadeh, Optik 127 (2016) 11433-11443; <https://doi.org/10.1016/j.ijleo.2016.09.013>
- [34] R. Hill, Proc. Phys. Soc., A 65 (1952) 349-354; <https://doi.org/10.1088/0370-1298/65/5/307>